

Effects of Gamma Radiation Versus Peroxide on Carbon Steel Corrosion

K. Daub, X. Zhang, J.J. Noël and J.C. Wren¹

¹ University of Western Ontario, London, Ontario, Canada
Chemistry Building 1151 Richmond St. N6A 5B7

Abstract

The effect of water radiolysis products produced by ionizing radiation on the corrosion kinetics of carbon steel has been studied at pH 10.6 and room temperature, using electrochemical and chemical speciation analyses. The present study investigates the effect of γ -radiation on carbon steel corrosion and compares it with that of chemically added H_2O_2 , which is considered to be the key radiolytically produced oxidant at room temperature. Various oxide films were pre-grown potentiostatically on carbon steel electrodes, and then exposed to either γ -radiation or H_2O_2 . The corrosion kinetics were studied by monitoring the corrosion potential (E_{CORR}), and periodically measuring the polarization resistance.

1. Introduction

Accurate understanding of the effects of ionizing radiation on nuclear reactor system chemistry and materials corrosion is important for assessment of various operational and maintenance requirements and safety margins of nuclear power plants. Exposed to ionizing radiation (e.g., gamma radiation), water decomposes into both oxidizing and reducing species, such as $\bullet\text{OH}$, H_2O_2 , O_2 , $\bullet\text{O}_2^-$, etc, whose net interactions with steels are not well characterized. In a constant radiation field, these radiolysis products achieve low, but steady-state levels and can dictate the aqueous redox condition, and, hence, may control corrosion reactions. However, since the radiolysis products are chemically reactive, their steady-state concentrations in the homogeneous solution phase can be easily affected by features of the aqueous chemical environment such as pH, temperature and the presence of other dissolved species. For example, during γ -radiolysis of water, there is an increase of more than two orders of magnitude in the production of H_2 and H_2O_2 when the pH increases from 6.0 to 10.6 [1,2]. Oxide film formation and conversion on carbon steel, and hence, the corrosion rate, are also strongly pH and potential-dependent [3]. This potential dependence of the carbon steel corrosion varies considerably with pH. Consequently, the net effect of water radiolysis on metal corrosion and corrosion product transport is often difficult to predict.

The influence of ionizing radiation on corrosion of metals in general, and, of carbon steel in particular, has been studied only to a limited extent, and the mechanism by which radiation affects corrosion kinetics has not been established [4-8]. The observed effects of ionizing radiation on the corrosion of metals are conflicting [4-15], and many key questions remain unanswered, including whether the radiation energy initially absorbed in the bulk metal phase, or that in the aqueous phase, is what drives materials degradation, and whether the key aqueous redox species for steel corrosion are the radical products or the molecular products from water radiolysis.

Previous studies on the effect of γ -radiation reported that the corrosion of carbon steel is enhanced by radiation exposure. However, most of these studies relied on very limited measurements such as the amounts of Fe^{II} and Fe^{III} ions released to the solution and later collected by filtration [4,5]

or on the weight loss of test coupons [6-8]. Electrochemical methods of monitoring surface changes during corrosion were not employed by these authors. Although the possibility that radiation-induced oxidation of dissolved Fe^{2+} ions is the dominant effect was also raised [2], these studies did not probe the role of water radiolysis products as redox agents that may dictate the film formation and conversion on carbon steel. Only Fujita et al. [7,8] attempted to examine the types of corrosion deposits formed on the metal surfaces, finding only magnetite by X-ray diffraction under their exposure conditions.

To develop a fundamental understanding of the effects of water radiolysis on system chemistry and materials degradation in nuclear reactor environments, a comprehensive program has been put in place, which includes studies on catalytic effects of dissolved chemical additives (corrosion products and pH- or redox-controlling agents) on water radiolysis and steel corrosion in aggressive redox environments that simulate radiolytically induced aqueous environments by chemical additions, as well as steel corrosion in a gamma-irradiation field.

This study investigates the effects of γ -radiation on carbon steel corrosion and compares them with those of chemically-added H_2O_2 that is considered to be the key radiolytically-produced oxidant at room temperature. The corrosion kinetics are monitored by measuring the corrosion potential, E_{CORR} , and the polarization resistance, R_p , using linear polarization (LP) and electrochemical impedance spectroscopy (EIS). Since surface morphology and composition, in addition to the change in the aqueous redox environment induced by γ -irradiation, are important factors controlling the corrosion rate, this study has been performed with various oxide films that were pre-grown potentiostatically on carbon steel electrodes prior to exposure to either γ -radiation at a dose rate of $\sim 6.8 \text{ kGy}\cdot\text{h}^{-1}$ or to H_2O_2 at concentrations in the range of 10^{-6} to 10^{-2} M .

2. Experimental

2.1 Electrochemical Cell

A three-electrode cell, consisting of a reference electrode, a Pt mesh counter electrode and a carbon steel working electrode, was used. In the case of all experiments conducted outside of the radiation environment, the reference electrode used was a saturated calomel electrode (SCE) (Fisher Scientific), whereas for radiation experiments a Hg/HgO reference electrode (Radiometer Analytical) in 1.0 M KOH solution was employed. The Hg/HgO electrode has been found to be more resistant to radiation than the saturated calomel electrode (SCE) or Ag/AgCl electrode, and has a potential of 0.112 V versus the Standard Hydrogen Electrode (SHE). All potentials are quoted on the SCE scale (0.242V vs. SHE). The working electrode in all experiments was A516 Gr70 carbon steel, purchased from Goodfellow (in wt%: C, 0.20; Mn, 1.05; Si, 0.32; Al, 0.04; P, 0.015; S, 0.008; balance Fe). Prior to each experiment, the working electrode was polished manually with 600 and 1200 grit silicon carbide papers, followed by polishing on a Texmet microcloth (Buehler) with a 1 μm MetaDi Supreme diamond paste suspension (Buehler), and lastly sonication in an acetone/methanol mixture for 5 minutes to remove polishing residues.

A Solartron model 1480 multistat and model 1255 frequency response analyzer were used in all electrochemical measurements. CorrwareTM and ZplotTM software (Scribner and Associates) were used for experiment control and data analysis. EIS was performed by applying a $\pm 10\text{mV}$ sinusoidal potential stimulus, either at the corrosion potential, E_{CORR} , or an applied potential, E_{APP} , while the analyzer converted the system response into an impedance value. The frequency was varied over the range 10^4 Hz to 10^{-2} Hz . A second frequency scan consisting of measurements at several frequencies

spanning the same range was then acquired to verify that the electrode surface remained at steady-state over the course of the EIS measurement. Linear polarization measurements were performed by scanning the potential from the corrosion potential to -0.015 V vs. the corrosion potential, then to $+0.015$ V vs. the corrosion potential, and finally back to the corrosion potential, at a rate of 0.1667 mV/s.

2.2 Solutions

All experiments were conducted at room temperature in Ar-sparged 0.01 M sodium borate solutions. The solutions were prepared using reagent grade $\text{Na}_2\text{B}_3\text{O}_7$ (Caledon Laboratories Ltd.) and water purified using a NANOpure Diamond UV ultra-pure water system (Barnstead International), with a resistivity of 18.2 M Ω -cm. Reagent grade NaOH (Caledon Laboratories Ltd.) was added dropwise to the solutions to adjust the pH. All experiments were conducted at a pH of 10.6. H_2O_2 was added from a 3 wt. % stock solution from Fisher Chemicals.

2.3 Irradiation Source

All irradiation experiments were conducted in a MDS Nordion Gammacell 220 Excel Cobalt-60 irradiator. The electrochemical cell was positioned inside the gammacell sample chamber, and the chamber was lowered into the gammacell irradiation zone, consisting of 11 tubular pencils containing ^{60}Co . The dose rate during the period of experimentation was ~ 6.8 kGy $\cdot\text{h}^{-1}$.

2.4 Procedure

Following application of the polishing procedures described previously (section 2.1), the working electrodes were rinsed with deionized water and placed in the electrochemical cell, which had been sparged with argon gas for at least 1 hour to purge any oxygen from the solution. Electrochemical experiments then began with cathodic cleaning at -1.1 V for 5 minutes to remove any residual air-formed oxides on the working electrode, thereby creating a virtually clean metal surface. The electrode was then anodized for 2.5 h at -0.7 , -0.2 , or 0.2 V with the intention of generating a variety of oxide films with differing compositions and properties. When the potentiostatic film growth was completed, either, the electrochemical cell was irradiated in the gammacell for 6 h, or a specific concentration of H_2O_2 was added to the solution; E_{CORR} was measured during the entire procedure. E_{CORR} monitoring continued for a number of hours (generally 24 to 48 h) to follow any changes occurring in solution and on the metal oxide surface.

Over the course of the experiments, periodic measurements of either EIS or LP were performed to aid in determining the change in the resistive nature of the oxide film. Also, to evaluate the radiolytic production of redox species, gaseous and aqueous samples were taken periodically for H_2O_2 analysis by UV-Vis spectrophotometry and for O_2 and H_2 analysis by gas chromatography.

In some cases, 24 h after the addition of H_2O_2 , carbon steel samples were removed and analyzed using X-ray photoelectron spectroscopy (XPS).

3. Results

3.1 Electrochemical Growth and Conversion of Oxide on Carbon Steel

The oxidation of carbon steel can be divided into three potential regions, identified in previous studies, [16,17].

In Region I ($E \leq -0.7$ V vs SCE), the main oxide formed is Fe_3O_4 , which grows via a solid-state process, except that in the very early stages of film formation highly soluble Fe^{II} oxides/hydroxides may be formed;

In Region II (-0.5 V $\leq E$ (vs SCE) ≤ -0.1 V), continuous growth of the Fe_3O_4 layer is accompanied by its anodic conversion to a more maghemite ($\gamma\text{-Fe}_2\text{O}_3$)-like phase near, or at, the oxide/solution interface by a similar solid-state mechanism; and

In Region III (0.0 V $< E$ (vs SCE) < 0.4 V), the anodic conversion of this $\text{Fe}_3\text{O}_4/\gamma\text{-Fe}_2\text{O}_3$ oxide to $\gamma\text{-FeOOH}$ leads to structural changes, which can induce micro-fracture. In the absence of aggressive anions, the surface quickly repassivates, and the layer of $\text{Fe}_3\text{O}_4/\gamma\text{-Fe}_2\text{O}_3$ can grow by continuous film fracture and repassivation, producing a thicker and more defective (or porous) oxide film.

3.1 Water Radiolysis Products in a γ -Irradiation Field

During the irradiation period, the electrolyte solution was also periodically sampled to determine the concentration of radiolytically-produced H_2O_2 , Figure 1.

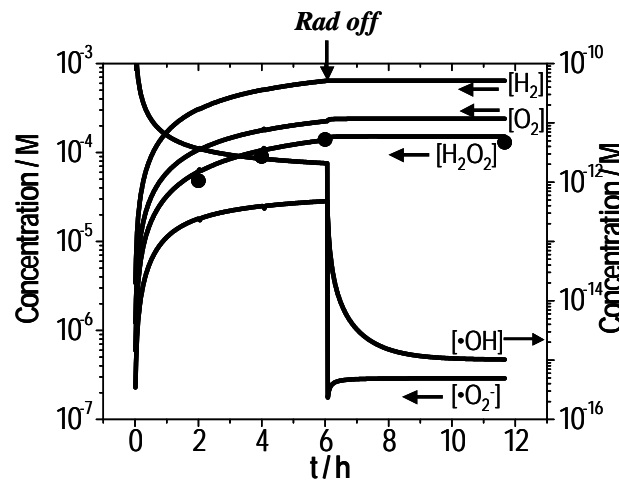


Figure 1: Concentration of water radiolysis products during and post 6 h irradiation. The lines indicate the calculated concentrations and the symbols represent the measured concentrations of H_2O_2 .

At pH 10.6 the radiolytic production of H_2O_2 does not reach steady state immediately, but the concentration gradually increases over the 6 h irradiation period, from $[\text{H}_2\text{O}_2] = \sim 10^{-6}$ M at 0.5 h to $[\text{H}_2\text{O}_2] = \sim 10^{-4}$ M at 6 h. In the figure, the measured H_2O_2 concentration is compared to that calculated using a water radiolysis model that has been tested under a wide range of conditions [1,2].

The model reproduces the measured $[H_2O_2]$ very well, and is used to aid interpretation of the behaviour of unstable (and hence not easily measurable) radical redox species ($\bullet O_2^-$, $\bullet OH$), whose calculated concentrations are also presented in Figure 1. The solution pH values measured before and after irradiation were the same (pH 10.6), confirming that the buffer solution was able to maintain the pH.

Although E_{CORR} is a complicated function of the nature of the oxide film as well as of the aqueous redox condition, the comparison of the time-dependent behaviour of E_{CORR} (Figure 2) and the radiolysis product speciation (Figure 1) suggest that under our experimental conditions (pH 10.6 and room temperature) the molecular products, not the radical products, are the main radiolysis products controlling E_{CORR} .

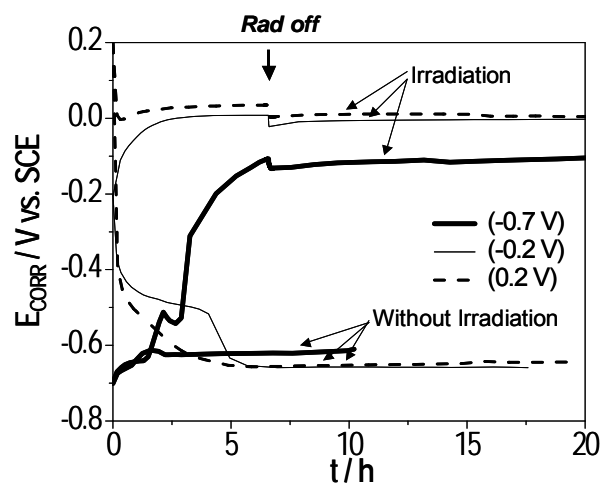


Figure 2: Corrosion potential as a function of time during and post 6 h irradiation and without irradiation. Prior to the E_{CORR} measurement, oxide films were grown potentiostatically at +0.2 V, -0.2 V, or -0.7 V.

During irradiation the concentration of $\bullet OH$ is several orders of magnitude lower than that of any of the molecular species, and even the more stable (and hence less reactive) superoxide radical $\bullet O_2^-$ is also an order of magnitude lower. Furthermore, upon the termination of irradiation, these radicals quickly decay to background levels, whereas no change in E_{CORR} is observed. These comparisons strongly suggest that it is the radiolytically-produced molecular species, in particular H_2O_2 , and not the radical species, that determines the E_{CORR} of carbon steel. This claim is consistent with the expectation for solid-liquid reactions, which, in general, have higher activation energies and lower reaction rates than bulk homogeneous solution reactions. Thus, the radical species would be more likely to recombine with other radical species or react with dissolved impurities, if present, than to be involved in surface oxidation and reduction reactions. From the radiolysis perspective, OH^- is an impurity that can considerably reduce the radical concentrations [1,2], and under our experimental conditions (pH 10.6) the ratio of molecular species to radical species is much higher than that expected for pH less than 8 [2].

3.2 Comparison of E_{CORR} During Exposure to γ -Radiation and to H_2O_2 .

In Figure 3, E_{CORR} during the exposure to γ -radiation is compared with E_{CORR} observed in solutions containing 1×10^{-6} M and 1×10^{-4} M H_2O_2 .

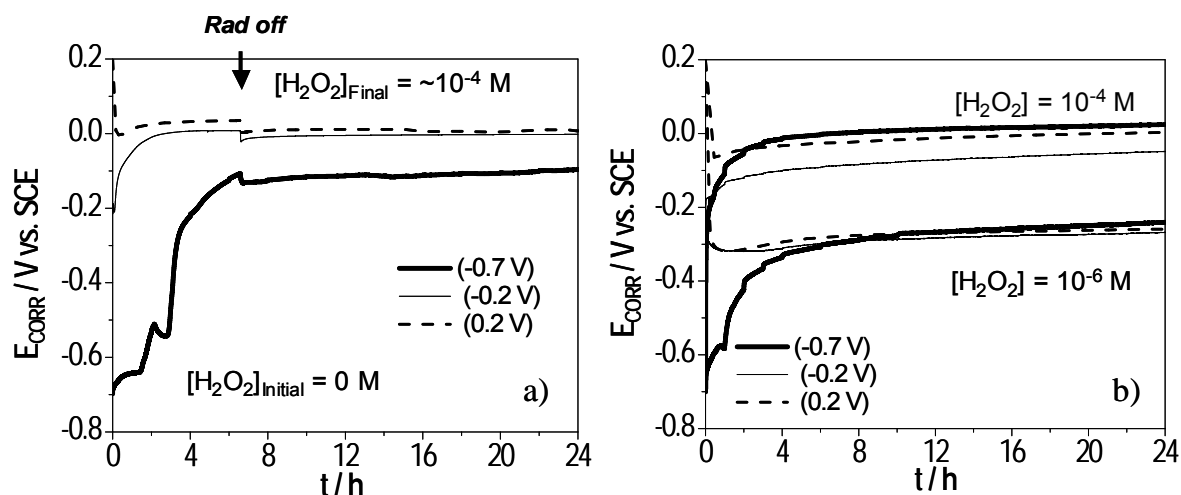


Figure 3: E_{CORR} observed a) during and after exposure to 6 h γ -irradiation; and b) during exposure to H_2O_2 for the films pre-grown at +0.2 V, -0.2 V, and -0.7 V. Two sets of data obtained in 10^{-4} M H_2O_2 and 10^{-6} M H_2O_2 are shown in b).

Considering the change in $[\text{H}_2\text{O}_2]$ with irradiation time (see Figure 1 showing $[\text{H}_2\text{O}_2]$ ranging from $\sim 10^{-6}$ M at 0.5 h to $\sim 10^{-4}$ M at 6 h), the E_{CORR} radiation results compare very well with the H_2O_2 results. The slower approach to steady state of E_{CORR} of the irradiated systems, compared to E_{CORR} of the 1×10^{-4} M H_2O_2 solution, is attributed to the gradual increase in $[\text{H}_2\text{O}_2]$ during irradiation. However, when the concentration of radiolytically produced H_2O_2 reached steady-state at $\sim 1 \times 10^{-4}$ M, the $(E_{\text{CORR}})_{\text{SS}}$ values of the irradiated systems are those observed in 1×10^{-4} M H_2O_2 solutions. The reason for the slightly lower E_{CORR} observed at the end of irradiation with the film pre-grown at -0.7 V is not clear. One explanation may be that due to the gradual increase in $[\text{H}_2\text{O}_2]$ during the 6 h irradiation E_{CORR} reaches a value in Region II at a later time, and once it reaches Region II E_{CORR} increases very slowly due to the passivity of the film formed in this potential region.

These results strongly support the claims that the key radiolytically-produced redox species is H_2O_2 and that E_{CORR} during and post γ -irradiation is reasonably well simulated by adding H_2O_2 of chemical origin at the time-dependent concentration levels achieved radiolytically. As was also seen, the system resistance behaviour observed under γ -irradiation conditions could also be simulated in a solution containing a representative concentration of H_2O_2 , further supporting the above claim.

Radiation dose rate also affects the steady-state concentrations; at a given pH the steady-state concentrations have a square root dependence on dose rate [1]. Since H_2O_2 is the key radiolysis product controlling carbon steel corrosion, but its concentration depends on the radiation dose rate, a more detailed investigation of the effect of $[\text{H}_2\text{O}_2]$ on carbon steel corrosion, in particular on the oxide film growth and conversion kinetics, has been performed.

3.3 Oxide Film Growth and Conversion in H_2O_2 Solutions

The steady-state E_{CORR} , R_p , and XPS studies all provided a consistent picture of the film conversion as a function of $[\text{H}_2\text{O}_2]$. At $[\text{H}_2\text{O}_2]$ ($< 10^{-3}$ M), E_{CORR} increased with an increase in

[H₂O₂], but its values remained within Region II. The film growth in this potential region consists of continuous growth of the conducting Fe₃O₄ layer accompanied by its anodic conversion to a more maghemite (γ-Fe₂O₃)-like phase near, or at, the oxide/solution interface [3,17]. The oxide formed is mainly a compact Fe₃O₄/γ-Fe₂O₃ layer whose growth is limited mainly by the dissolution rate of the oxide, and, to a smaller extent, E_{CORR}. This oxide formation mechanism can thus explain the small increase in film resistance with [H₂O₂], Figure 4.

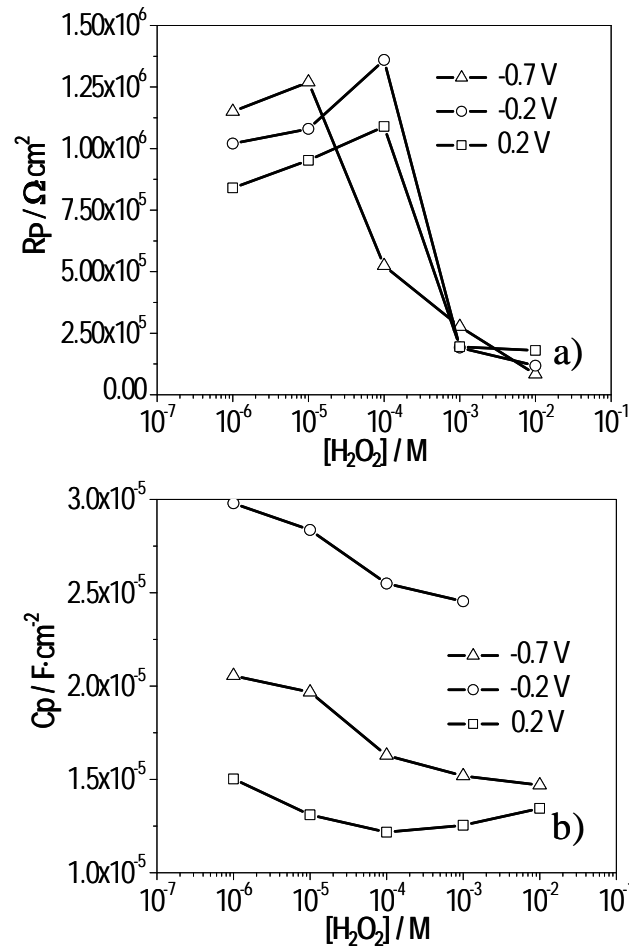


Figure 4: Steady-state a) polarization resistance and b) capacitance as a function of added H₂O₂ for the films pre-grown at (□) +0.2 V, (O) -0.2 V, and (Δ) -0.7 V.

This result is also consistent with the observation from the previous study [3] which showed that the resistance of the film grown over 7 days increases only slightly with the film growth potential in Region II. The XPS results showed a negligible change in the ratio of Fe^{III} oxides to Fe₃O₄ with increasing [H₂O₂], further support the thickening of Fe₃O₄/γ-Fe₂O₃ layer in the lower [H₂O₂] range.

At [H₂O₂] ≥ 10⁻³ M, E_{CORR} (Figure 5) was at the cusp of Region III, where the anodic conversion of this Fe₃O₄/γ-Fe₂O₃ oxide to γ-FeOOH can lead to micro-fracture and the layer of Fe₃O₄/γ-Fe₂O₃ can grow by continuous film fracture and repassivation, producing a thicker and more defective (or porous) oxide film [3,17].

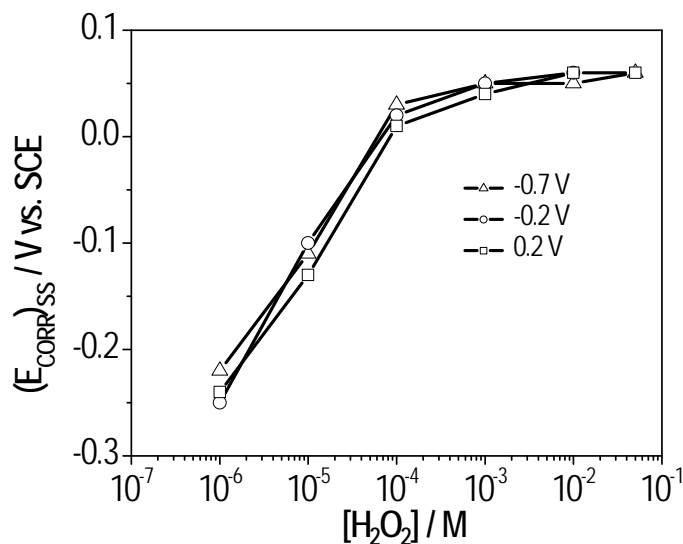


Figure 5: Steady-state E_{CORR} as a function of $[\text{H}_2\text{O}_2]$ for the films pre-grown potentiostatically for 2.5 h at -0.7 V, -0.2 V, and $+0.2$ V for 2.5 h.

This mechanism is consistent with the XPS results showing a higher ratio of Fe^{III} oxides to Fe_3O_4 at $[\text{H}_2\text{O}_2] \geq 10^{-3}$ M. It has been shown while in the presence of aggressive anions the film fracture can lead to pitting corrosion, in their absence the film quickly passivates and does not result in pitting [3,17]. The EIS or the SEM of the carbon steel electrodes exposed to high $[\text{H}_2\text{O}_2]$ did not show any sign of pitting corrosion (results not shown). Irrespective of the exact nature of the Fe^{III} oxides, high R_P values are expected if the polarization resistance obtained by EIS is determined by the charge transfer resistance on the film surface. This is what was observed in the absence of H_2O_2 [16,17], where high R_P values were observed for the films grown electrochemically in this potential range. Thus, the significantly lower resistance observed at $[\text{H}_2\text{O}_2] \geq 1 \times 10^{-3}$ M is attributed not to a breach of film passivity, but to surface-catalyzed H_2O_2 decomposition coupled with the $\text{Fe}^{\text{III}}/\text{Fe}^{\text{II}}$ electron donor-acceptor relay, (i.e., electronic, not ionic, conductivity increases and enhances H_2O_2 decomposition). The claim is further supported by the independence of E_{CORR} on $[\text{H}_2\text{O}_2]$ (Figure 5) and the increase in the Fe^{III} oxides composition in the film (XPS) at $[\text{H}_2\text{O}_2] \geq 10^{-3}$ M.

The steady-state E_{CORR} and R_P show negligible dependence on the type of pre-grown film. The nature and thickness of the pre-grown film appear to affect the initial kinetics of the film conversion and the time to reach steady state. For both E_{CORR} and R_P , the time to reach steady state is longest for the film pre-grown at -0.2 V, as expected, since the pre-grown film would be composed of a more passive and compact $\text{Fe}_3\text{O}_4/\gamma\text{-Fe}_2\text{O}_3$ layer.

4. Conclusions

The effects of γ -irradiation and of H_2O_2 on carbon steel corrosion at pH 10.6 and room temperature were investigated by E_{CORR} , EIS, and LP measurements. Both E_{CORR} and R_P behaviour under radiation conditions could be simulated in a solution containing a representative concentration of H_2O_2 , indicating that H_2O_2 is the key radiolysis product controlling carbon steel corrosion.

Both the steady-state E_{CORR} and R_P are strong functions of $[\text{H}_2\text{O}_2]$, but nearly independent of the initial oxide film composition. The E_{CORR} and R_P behaviour showed two distinct ranges dependent

on $[H_2O_2]$. For $[H_2O_2] < 10^{-3}$ M, E_{CORR} is determined mainly by the cathodic half-reactions of H_2O_2 to yield OH^- , coupled with the anodic half-reactions of the oxide-covered steel surface. On the other hand, for $[H_2O_2] \geq 10^{-3}$ M, E_{CORR} is likely to be determined primarily by the cathodic half-reactions of H_2O_2 , coupled with the anodic half-reactions of H_2O_2 .

This study clearly illustrates that the corrosion rate of carbon steel in a γ -radiation environment at pH 10.6 and room temperature can be predicted from the dependence of E_{CORR} and R_p on $[H_2O_2]$ if the concentration of radiolytically-produced H_2O_2 can be determined or measured.

5. Acknowledgments

This research was funded under the Natural Science and Engineering Council of Canada (NSERC) and Atomic Energy of Canada Limited (AECL) Industrial Research Chair Agreement. The electrochemical analysis equipment was purchased by a grant from the Canada Foundation for Innovation.

6. References

- [1] J. M. Joseph, B.S. Choi, P. Yakabuskie, J. C. Wren, *Radiat. Phys. Chem.* 77 (2008) 1009.
- [2] P. Yakabuskie, J.M. Joseph, J.C. Wren, Submitted to *Radiat. Phys. Chem.* (2009). Accepted.
- [3] W. Xu, K. Daub, X. Zhang, J.J. Noel, D.W. Shoesmith, J.C. Wren, *Electrochim. Acta* 54 (2009) 5727.
- [4] S. Neufuss, V. Cuba, R. Silber, V. Mucka, M. Pospisil, A. Vokal, *Czech. J. Phys.* 56 (2006) D365.
- [5] K. Ishigure, N. Fujita, T. Tamura, K. Oshima, *Nucl. Technol.* 50 (1980) 169.
- [6] T.E. Gangwer, K.K.S. Pillay, *Nucl. Technol.* 58 (1982) 548.
- [7] N. Fujita, C. Matsuura, K. Saigo, *Radiat. Phys. Chem.* 58 (2000) 139.
- [8] N. Fujita, C. Matsuura, K. Saigo, *Radiat. Phys. Chem.* 60 (2001) 53.
- [9] N. Fujita, C. Matsuura, K. Saigo, *Radiat. Phys. Chem.* 49 (1997) 357.
- [10] N. Fujita, C. Matsuura, K. Saigo, *Radiat. Phys. Chem.* 50 (1997) 457.
- [11] T. Yamamoto, S. Tsukui, S. Okamoto, T. Nagai, M. Takeuchi, S. Takeda, Y. Tanaka, *J. Nucl. Mater.* 228 (1996) 162.
- [12] W.E. Clark, *J. Electrochem. Soc.* 105 (1958) 483.
- [13] G.P. Marsh, K.J. Taylor, G. Bryan, S.E. Worthington, *Corros. Sci.* 26 (1986) 971.
- [14] R.S. Glass, G.E. Overturf, R.A. Van Konyenburg, R.D. McCrigh, *Corros. Sci.* 26 (1986) 577.
- [15] Y.J. Kim, K.J. Oriani, *Corros.* 43 (1987) 92.
- [16] X. Zhang, W. Xu, D.W. Shoesmith, J.C. Wren, *Corros. Sci.* 49 (2007) 4553.
- [17] K. Yazdanfar, X. Zhang, P.G. Keech, D.W. Shoesmith, J.C. Wren, *Corros. Sci.* 52 (2010) 1297.